

On the simulation of molded micro components and systems

Albert Albers · Hans-Georg Enkler ·
Pablo Leslabay

Received: 15 June 2007 / Accepted: 16 December 2007 / Published online: 5 March 2008
© Springer-Verlag 2008

Abstract Regarding micro components and systems, experimental work for characterizing materials' properties as well as components' and systems' behaviors have to be supplemented by numerical analyses. These analyses should cover component and system issues. On a component level, macroscopic approaches are extended by methods allowing consideration of the influence of components' grain structures including possible defects. On a system level, the high tolerances accepted for the individual components due to production inaccuracy and their effects on the expected load distribution capability of the system are taken into account. This paper presents approaches for simulation of micro components and systems using the finite element method and multi body simulation. Methods to overcome the abovementioned issues will be shown, as well as the effects of grain structure on the stress distribution in the individual components.

1 Introduction

The development of smaller and smaller micro components and systems is an ongoing process. Within the scope of Collaborative Research Center 499 "design, production and quality assurance of molded micro components made of metallic and ceramic materials" fundamentals in a persistent process chain for micro components are acquired. As a participating member, the Institute of

Product Development is dealing with the development, design and dimensioning of micro components.

Regarding micro components and systems, experimental work for characterizing materials' properties as well as components' and systems' behaviors have to be supplemented by numerical analyses. These analyses should allow examining specific influences on the mechanical stress. In the macroscopic world finite element method (FEM) (Zienkiewicz and Taylor 2005) and multi body simulation (MBS) (Shabana 2001) have been established as a reliable tool throughout the product development process. By means of FEM and MBS, virtual components and systems can be set up, stress distributions, contact and dynamic forces can be acquired, and variations can be compared, even before a prototype exists. However, when advancing to dimensions of micro technology effects negligible in the macroscopic world may occur. Regarding micro technology, these effects as well as applicability of the aforementioned numerical methods have to be investigated.

2 General approach

General goal of this work is a persistent virtual process, i.e., for consideration of micro specific effects a computer-aided simulation tool is being developed. This tool supplements established analysis software, e.g., FE analyses of micro components are based on established FE solvers. It is aimed for an automatable procedure that enables posterior sensitivity analyses, for example. On a system level, contact forces and positions are examined for relevant geometric variations resulting from production, abrasion, etc. A component level allows investigation of stress, strain and flow of forces at different operating conditions with

A. Albers (✉) · H.-G. Enkler · P. Leslabay
Institute of Product Development (IPEK),
University of Karlsruhe (TH), 76131 Karlsruhe, Germany
e-mail: albers@ipek.uni-karlsruhe.de

respect to the grain structure. Effects and restrictions of those levels are considered among one another. Figure 1 shows this simulation process.

3 Modeling of components

Decreasing systems' and therefore components' size while simultaneously increasing loads necessitates, amongst others, computational analyses. Yet, approved techniques in macro dimensions cannot always be scaled down to micro dimensions. Usually, FEM analyses proceed from the assumption of isotropic material behavior. This assumption does not apply implicitly when simulating micro components. With decreasing size of a component its grain structure and material anisotropy gain more and more influence on its mechanical stress distribution and flow of forces (Fröhlich et al. 2001). Thus, a geometric model of the polycrystalline micro component that is close to reality has to be created.

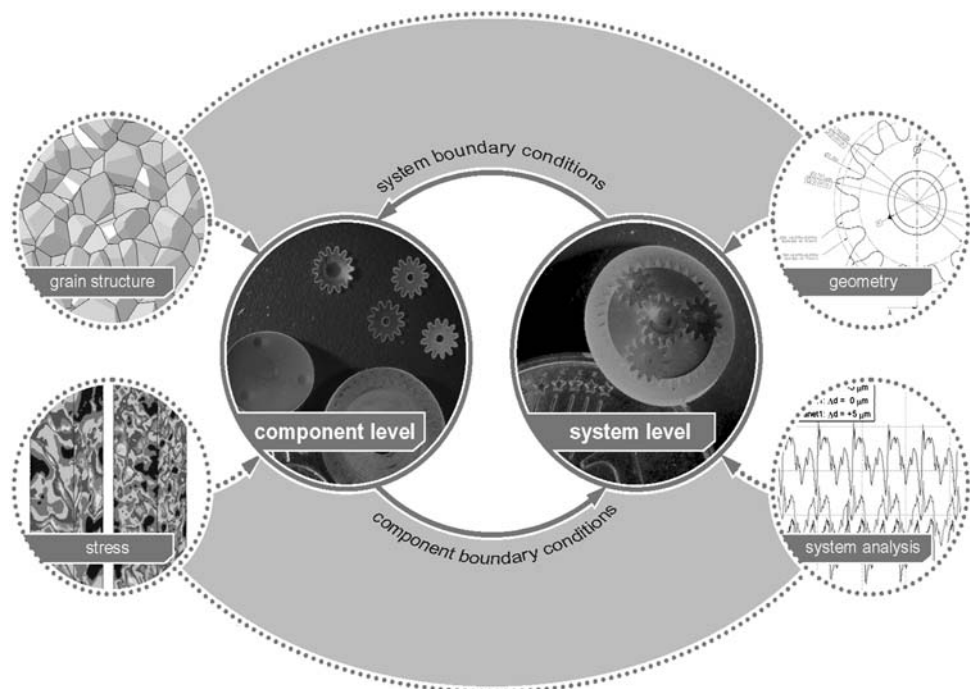
3.1 Modeling methods

One possibility is to model the grain structure by ordinary regular geometries such as squares (McMeeking and Hwang 1999). But the high degree of symmetry offers only limited applicability for irregular polycrystals. Another possibility would be to assume each Finite Element to represent a grain. However, mesh and grain size then are directly interdependent. For this reason, methods of

stochastic geometry are used. One of the most established methods is the Voronoi (1908) tessellation. The works of (Fröhlich et al. 2001; Albers and Metz 2005, 2006; Nygård 2003) for instance, are based on this method to generate a grain structure inside of a two-dimensional rectangular space. Voronoi tessellation decomposes a given space, e.g., by a discrete set of points, to a discrete set of objects within this space. The decomposition is thereby determined by distances. An overview of applicabilities is given in (Stoyan et al. 1995). The Voronoi tessellation directly results in a space completely filled with cells. These cells can be regarded as grains. Since the space is completely filled by them, pores and further defects have to be added afterwards and grain growth is not taken into account. For simulation of the formation of grain structures, cellular automata can be applied (Reher 1998; Bäker 2002). This offers great freedom depending on which formation processes should be taken into account in detail. One possibility is to start with a number of random points within a grid. At each step, adjacent grid points interact with each other. Grid points that are not yet assigned to a grain get part of it when it is adjacent to an already assigned element. Step by step, a structure develops. Even a simple model is able to provide fairly good results.

For this work, FE based method is applied (Albers and Enkler 2007). By means of FE based method, a grain structure is generated by mapping distance determined growth onto finite elements. For this reason, it is based on an existing FE mesh. When porosity takes zero as value, a discrete Voronoi structure is formed. Figure 2 shows two

Fig. 1 General approach



exemplary grain structures. Grain size distributions and further details can be evaluated so that parameters of the virtual grain structure can be validated by real ones.

The method offers good possibility for an automatized generation of grain structures. Therefore, parameters for generating the grain structure are determined in an additional input file. This file includes details on the grain structure, e.g., number of grains or growth rate.

In general, subdivision of a given space S into n grains necessitates that the grains do not penetrate each other and take in the whole space at least after the last iteration. Starting from n points according to the number of grains Eq. (1), a set $G(x_i)$ consisting of points whose distance to x_i is less or equal than to any other points of set G is assigned to each point in Eq. (2). The points of set P are called seeds.

$$P = \{x_1, x_2, \dots, x_n\} \subset S \tag{1}$$

$$G(x_i) = \bigcap_{x_j \in P \setminus \{x_i\}} \{y \in S \mid \|y - x_i\| \leq \|y - x_j\|\} \tag{2}$$

an algorithm for grain growth enables virtual grain growth by assigning the finite elements to the given seeds. Though, above-mentioned conditions are kept. Considering a given number of grains n , total volume $V_{a,t}$ taken by grains at a specific time t results from Eq. (3), where $m_{i,t}$ is the number of elements belonging to grain i at time t

$$V_{a,t} = \sum_{i=1}^n \sum_{j=1}^{m_{i,t}} V_j. \tag{3}$$

The porosity ϕ_t can be evaluated by Eq. (3) and total volume V_c of the component consisting of k elements, by the proportion of non-solid volume to total volume of material Eq. (4)

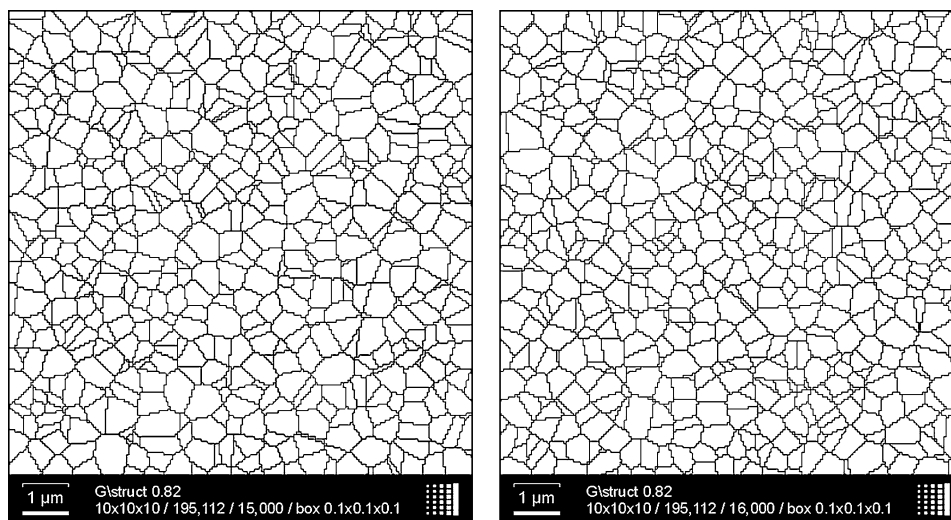
$$\phi_t = 1 - \frac{V_{a,t}}{V_c}, \quad V_c = \sum_{k=1}^p V_k. \tag{4}$$

3.2 Crystallographic orientation

The grains are considered as single crystals with anisotropic elastic behavior. The model of the material behavior is based on some assumptions. On the one hand, the modeled grains are assumed to be large enough, i.e., they have a sufficient volume that allows description by continuum mechanics. On the other hand, the grains themselves are assumed not to comprise failures. There-with, material properties can be described by ideal single crystal parameters. Furthermore, adjacent grains' orientations are independent. Eulerian Angles are used for characterization of the orientation of the crystals (Bunge 1982). The rotation matrix according to (Z, X', Z') convention is shown in Eq. (5)

$$R = \begin{pmatrix} \cos \psi \cos \phi - \cos \theta \sin \phi \sin \psi & -\sin \psi \cos \phi - \cos \theta \sin \phi \cos \psi & \sin \theta \sin \phi \\ \cos \psi \sin \phi + \cos \theta \cos \phi \sin \psi & -\sin \psi \sin \phi + \cos \theta \cos \phi \cos \psi & -\sin \theta \cos \phi \\ \sin \psi \sin \theta & \cos \psi \sin \theta & \cos \theta \end{pmatrix}. \tag{5}$$

Fig. 2 Virtually generated grain structures



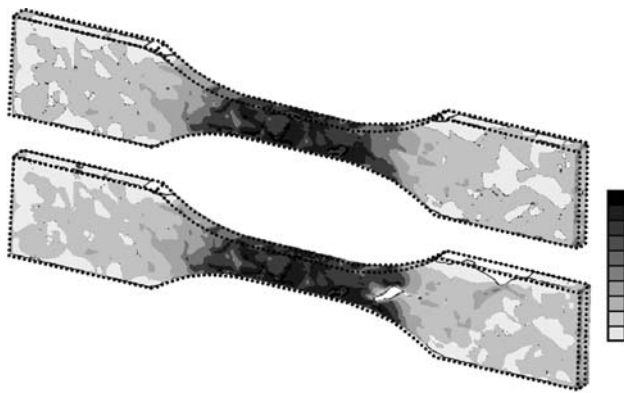


Fig. 3 Von Mises stress within a micro tensile specimen with grain structure; lower specimen containing a pore on the *right* hand side

3.3 Additional modeling and time effort

Particularly with regard to running multiple analyses each with different grain structures, e.g., for sensitivity analyses, additional effort in time for modeling of the grain structure has to be taken into account. Extent of this time depends on parameters such as number of seeds (Albers and Enkler 2007). In addition, time for solving the problem also exceeds assimilable conventional isotropic analyses due to increased complexity. In general, time effort coming along with consideration of the grain structure cannot be concealed but stays manageable and can be pre-estimated.

Applied methods are described in (Albers and Enkler 2007a, 2007b) in more detail.

Figure 3 exemplarily shows Von Mises stress within two tensile specimens. The lower specimen contains a pore. Using this algorithm, components with grain structures are modeled and analyzed on a system level.

4 Investigations on the system level

4.1 Studying the effects of tolerances and clearance on the overall system behavior

High precision and very tight tolerances are commonly assumed properties for micro components, at least for a range of manufacturing processes and materials. But it is not the only reality in the micro world. The production of metallic and ceramic micro molded components is still in its research-phase, and the components obtained by now are still wide tolerated. Thus, systems created with them have to accommodate these wide tolerances, and are therefore designed with significant clearance between the elements. Therefore, a study of the effects of this tolerance and clearance is needed, to understand and forecast the limits of such systems. The work was started with ordinary

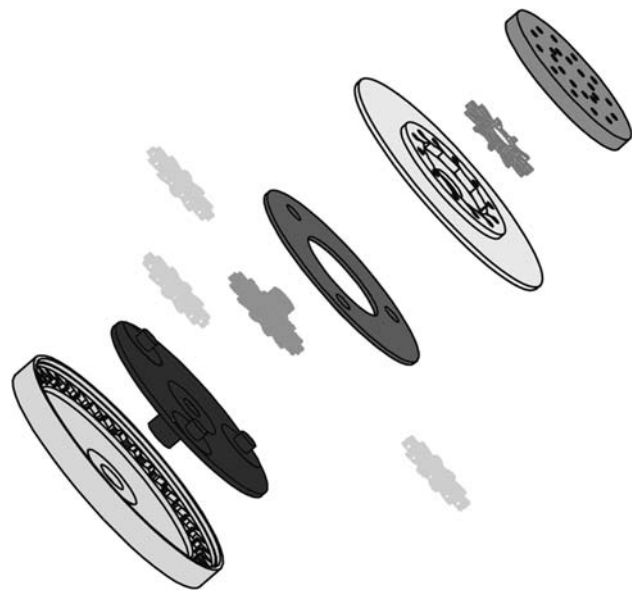


Fig. 4 Demonstratory one stage turbine and planetary gear train of the CRC499

MBS tools, and other techniques have then been adopted to further research details of the systems behavior.

For the rest of the work, a demonstrator consisting of a one-stage planetary gear train is taken as test case. As shown in Fig. 4, the planetary gear has a sun-planet-ring configuration. Table 1 gives insights about the geometry of the demonstrator.

4.2 Variation of geometrical parameters

The first of the geometrical parameters studied involves the position of the planets on the carrier. Variations have been conducted between the tolerance limits for the radial and tangential position of one planet. The results for the tangential variation on Fig. 5 show an increment of as much as 300% on the load for the ill-positioned planet, being milder (130%) for the radial variation.

Size variation in the planets within a gear train has also been studied, showing that the bigger of the planets tends to take most of the load in the system, similar to what happens by the pin position error.

Table 1 Geometrical configuration of the planetary gear train

	Sun	Planet	Ring	Carrier
Modulus (mm)	0.169	0.169	0.169	5.64
Z	14	12	37	1
Depth (mm)	0.156	0.156	0.200	0.140
Mass (mg)	5.54	2.79	–	24.73

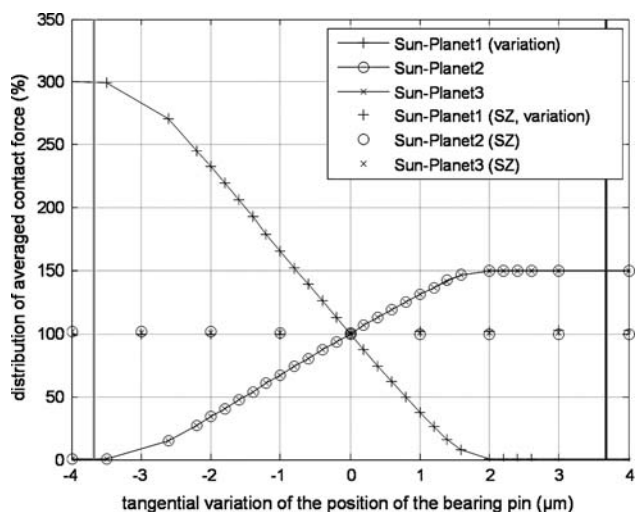


Fig. 5 Load variation between planets due to an error on the tangential position of the pin on the carrier. The *vertical continuous lines* show the tolerance limits

Clearance on the planet-carrier bearing and on the sun-case bearing has been varied within the tolerance range. Results show no effect due to the sun bearing, indicating that the clearance is bigger than needed, and a rising in the overload on the affected planet as the clearance between planet and carrier decreases.

Variation on the position of the centre hole of the planet has also been studied, but its effect is being absorbed by the clearance in the planet-carrier bearing.

A complete sensitivity analysis, running on a scriptable simulation tool, is being done to determine the influence of all of the known parameters on this demonstrator system, and to evaluate which of them are the most relevant to further investigate their effects.

4.3 Difficulties on simulating in small dimensions

The simulation of micro parts presents some particular difficulties to the multi-bodies dynamic solver, which need to be taken into account to successfully simulate the system.

An in-house study shows that the contact formulation of MBS software works best with body-penetration values between 1 μm and 500 μm. Unfortunately, the real values for materials and loads involved in this test case lie under the low-limit border, but the careful use of indentation on the spring constant has been proved helpful. The main disadvantage of indentation is the non-linear response introduced. Equation (6) shows the contact formulation implemented in the software:

$$f_n = k\delta^{m1} + c \frac{\dot{\delta}}{|\dot{\delta}|} |\dot{\delta}|^{m2} \delta^{m3}, \tag{6}$$

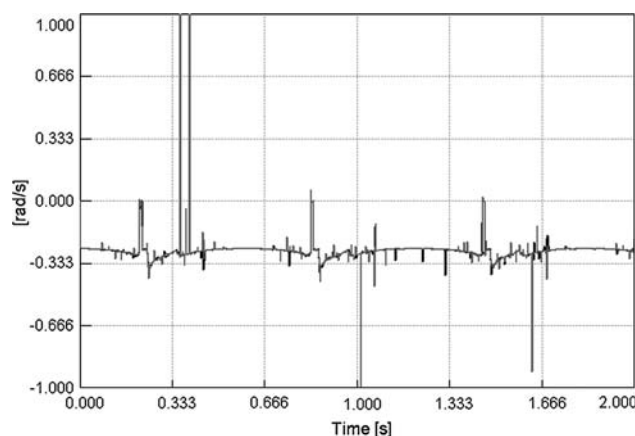


Fig. 6 The use of excessive small time steps can introduce unwanted high-frequency noise into the dynamic solution

where k, c are the spring and damping coefficients; $m1, m2$ and $m3$ are stiffness, damping and indentation exponents; δ a penetration and $\dot{\delta}$ a time differentiation of it.

Because some simulation tools set the zero value at 1e-08, an adequate and consistent system of units has to be selected on the software (or applied by the user if the software works dimensionless) in order to avoid “near zero” dynamic parameters. For example, the rotational inertia of the planets about their rotation axis is 1.52e-06 kg mm², but only 1.52e-12 kg m².

The simulation step width Δt is not only a matter of trouble on the direct integration of the dynamic equations. The best choice from an energetic point of view is to resolve the contact problem with steps as small as possible. If the steps are too big, non-physical effects like a ball bouncing higher than its start height on a free-fall problem can occur. These are pure numerical errors that disappear when Δt is properly selected. But solving with too small time steps has not only the disadvantage of being computer/time intensive. It is also possible that the calculated contact forces become contaminated with high frequency peaks that do not alter the overall trend of the response, but complicate the numerical evaluation of this force. An example of the implications of such noise is shown in Fig. 6. It is advisable to test the solver response to the contact problem with simple bodies of the same characteristic size as the contacting surfaces on the model, prior to starting long simulations.

5 Studying the stress state of the dynamic model

If it is desired to study the load and stress distribution within the moving parts of the system, the classical MBS

approach is no longer suitable. Traditionally, some FEM solvers have incorporated algorithms that allow them to work with rigid body motions and mechanisms (Bathe 1996). If the solver is not prepared to deal with this issue, a typical “The system matrix has negative eigenvalues” error will appear, and the simulation will stop.

Within the scope of the FEM for the structural dynamics analysis (Cook et al. 2002), this work will concentrate on the time-varying response (usually known as Response History) to loads applied softly and non-periodically, as in gear meshing, or suddenly as in impacts due to clearance. The issues about natural frequencies and steady-state response to harmonic loading are left to further research.

The frequency domain (or modal based) methods for achieving a Response History are best suited for linear problems, and have time advantages for multiple load cases. These methods are in most of the applications the fastest under the Response History methods (Belytschko 1976, 1983). In our case study, the deformation of the individual bodies remains small, and there is no plastic description of the material. But the necessary presence of contact surfaces on the gear teeth makes the study a non-linear case, and therefore not suitable for the modal approach.

A direct integration method is then needed (Cook et al. 2002; Crisfield 1991). Direct integration means the successive solving of the dynamic Eq. (7) at n instants of time separated by time increments Δt

$$[M]\{\ddot{D}\}_n + [C]\{\dot{D}\}_n + [K]\{D\}_n = \{R^{\text{ext}}\}_n. \quad (7)$$

6 Direct integration methods

There are mainly two different integration methods to solve this problem: the explicit and the implicit.

6.1 The explicit approach

An explicit algorithm uses a difference expression of the general form:

$$\{D\}_{n+1} = f(\{D\}_n, \{\dot{D}\}_n, \{\ddot{D}\}_n, \{D\}_{n-1}, \dots). \quad (8)$$

This is then mostly implemented in the central differences form

$$u_{n+1}^N = u_n^N + \Delta t_{n+1} \dot{u}_{n+\frac{1}{2}}^N \quad (9)$$

the method is called explicit in the sense that the kinematic state is advanced using known values of velocity and acceleration from the previous increments. The big computational advantage that can be won when properly implementing Eq. (9) in the explicit method is withdrawn by the fact that the method is conditionally stable, so there

is a maximum Δt that can be used, Δt_{crit} , to assure the convergence of the algorithm. Δt_{crit} is deeply related with the wave propagation velocity in the material, and can be well estimated by the CFL condition (Courant et al 1928; Isaacson and Keller 1966), where L is the length of the smallest element side, E the Young's Modulus and ρ the density.

$$\Delta t_{\text{crit}} \leq \frac{L}{\sqrt{\frac{E}{\rho}}} \quad (10)$$

in the case of micromolded components, the combination of small dimensions of parts and mesh, and very rigid materials, leads to very small Δt_{crit} , in the range of 1–3e-09 s, thus making the method impractical. Simulations conducted took more than 2 days to complete, even when the use of coarse meshes rose the Δt_{crit} to about 2e-07. Despite the good quality of the achieved results, this simulation method is not advisable for this problem, where the desired simulation time is many orders of magnitude longer than the wave propagation time.

6.2 The implicit approach

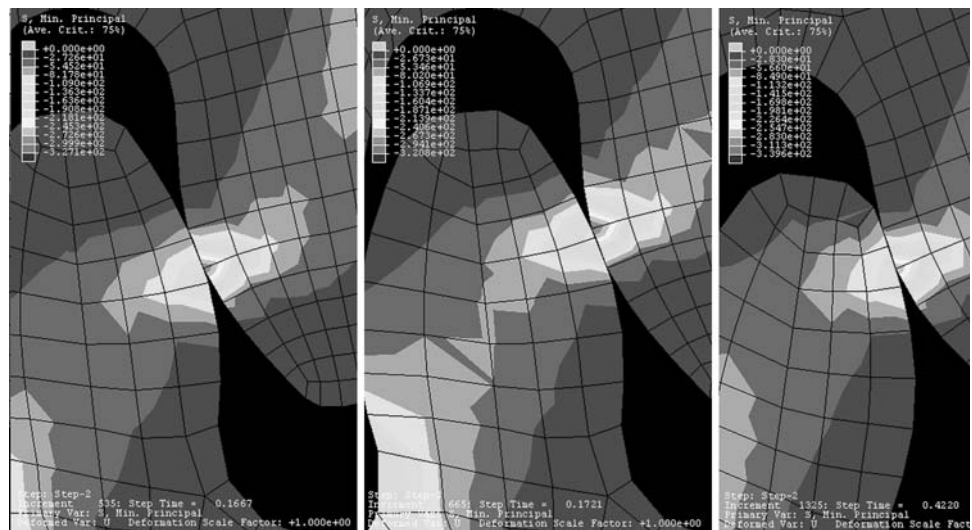
An implicit algorithm uses a difference expression of the general form:

$$\{D\}_{n+1} = f(\{\dot{D}\}_{n+1}, \{\ddot{D}\}_{n+1}, \{D\}_n, \{\dot{D}\}_n, \{\ddot{D}\}_n, \dots) \quad (11)$$

there are many implementations of the implicit algorithm, and all of them are or can be made unconditionally stable (Bathe 1996; Newmark 1959; Hilber et al. 1977; Hughes 1983) so the only limitation for the Δt is the quality of the computed results. On the other hand, the presence of the velocity and the acceleration vectors of the actual step in the computation of the displacements, forces simultaneous solving of Eq. (11), thus making the problem almost as slow as the series of static computations.

The implicit simulation trials using a commercial solver showed a difficulty with the contacting surfaces, which prevents the development of its full potential. The solver works stable at Δt as big as 5e-04 s, until it reaches a contacting point where two nodes of the same surfaces exchange load, see Fig. 7. There, the contact formulations request much smaller steps, until it comes through this “switching point”. But as the used solver is not able to roll-back more than the actual step in case of non convergence, using a long Δt for the trouble-free zone leads to a too “fast” entering onto the switching zone. In this situation, the algorithm is not able converge anymore, and the simulation stops. A reduction of the maximal Δt to 1.5e-04 s was needed to overcome the problem, producing a noticeable loose of efficiency in the implicit solver.

Fig. 7 The switching point problem. The solver needed 130 iterations to advance 0.0054 s from a to b (through the switching zone), then it took 660 iterations to advance 0.25 s



Simulation times of over 15 h are not good enough to try the statistical analyses needed for the desired grain structure modelling.

7 Studying the stress state due to part’s grain structure on the dynamic model

7.1 Adopting a quasi-static method

Further investigation of the influence of dynamic forces on the overall stress state of the individual gears confirmed their (at this point) expected small significance. The contribution on the principal stresses for a gear train accelerating from 0 to 10,000 RPM in 0.1 s, for a gear train rotating at 10,000 RPM and for both loads acting simultaneously are summarized on Table 2.

For small acceleration and inertial contributions, the effects of impact can be simplified and modelled as the superposition of the external loads and the momentum due to the velocity difference between the contacting bodies. The effects of friction have been neglected on this work, linear material models have been adopted, and bearing damping has been kept as low as possible. Under these

Table 2 Max principal stress due to different unloaded dynamic states of the system

Load case	Acceleration (Mpa)	Inertial (Mpa)	Simultaneous (Mpa)
Sun about centre	1.40e-04	5.56e-03	5.56e-03
Planet About centre	3.82e-04	1.77e-02	1.99e-02
About sun	1.34e-04	2.51e-03	

assumptions, it is reasonably to transform this dynamic problem into a series of static situations. The main advantage of doing so is that the Δt can now be selected freely, although it has lost most of its significance. This transformation allowed setting up reasonably low simulation times, which then allowed conducting the statistical analyses required for part’s grain structures.

7.2 Statistical analyses of grain structures

The study has been conducted for 2D and 3D grain structures, although the movement remained always planar due to the revolute joints used on the 3D simulations. The motivation for “extruding” the 2D model into 3D one laid

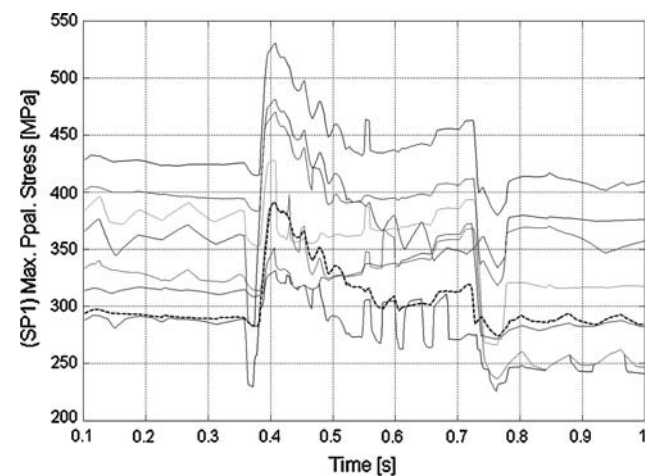


Fig. 8 Sample of result curves for the grain structure 3. The upper and lower curves are the envelope of max and min values, the dotted curve is the result of an isotropic simulation, the middle curves are individual simulation results

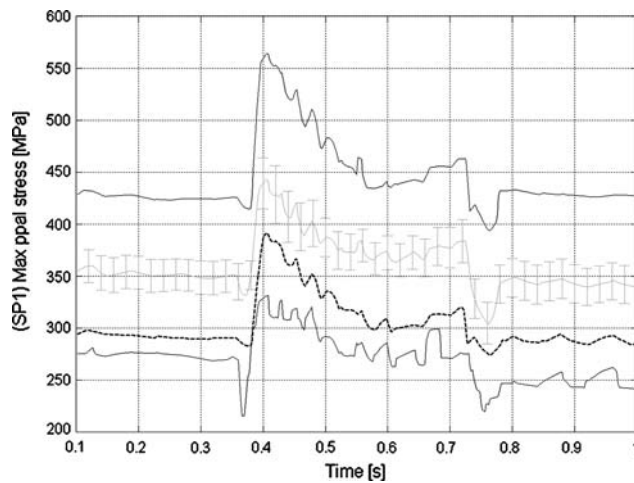


Fig. 9 Envelope curves for all the 150 2D cases, the isotropic results, and the mean value of the cases. The *columns* show the standard deviation of the results

on interesting effects detected on the bearings for the 2D model. As shown in the 3D results in Fig. 11, the non-isotropy of the grain structure alters the uniform distribution of the contact forces along the axial direction of the teeth, thus generating resultant forces tending to turn the gears out of the rotation plain.

The 2D simulations have been conducted for 3 different grain structures with 182, 211 and 212 grains. Each of them has been computed 50 times with different material orientations, generating 150 different grain structure cases. A single 3D grain structure with 400 grains has been computed for 40 different material orientations.

In the following Figs. 8, 9, 10, 11, the effects of the part's grain structure on its maximal principal stresses, the

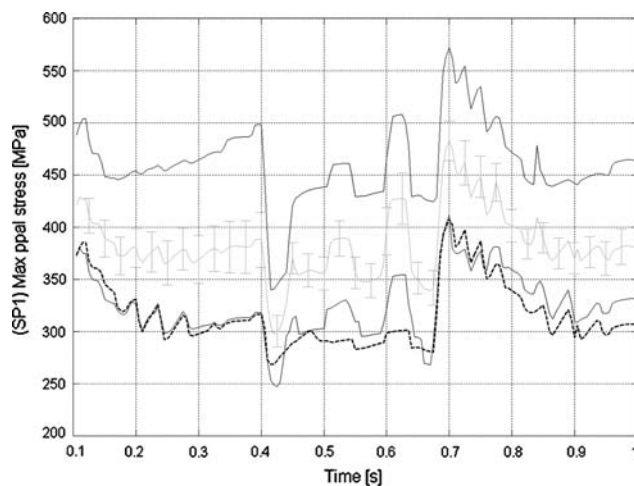


Fig. 10 Envelope curves for all the 40 3D cases, the isotropic results, and the mean value of the cases. The *columns* show the standard deviation of the results

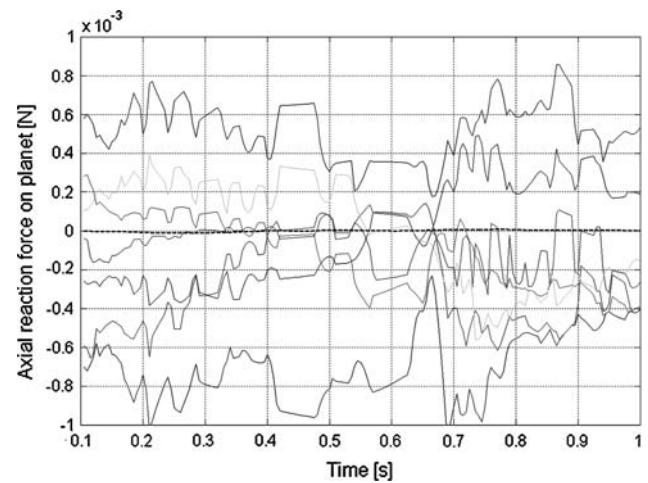


Fig. 11 Results for the axial reaction force on the planet revolute joint. Same curve structure as Fig. 8. As expected for the isotropic simulation, the force is null

variation of the reaction forces and the appearance of out-of plane forces due to anisotropy are shown.

The stability on the iteration number and CPU-time needed by the solver for each case reveals that all the simulations were able to run under identical conditions, thus showing that the effects appeared on the contact surfaces are only caused by the grain structure and not introduced by numerical issues. Table 3 summarizes the resulting values. The locations of the highest stressed elements remained also concentrated, but on different zones for each test case, and accompanied the teeth's gearing as each simulation advanced in time. Both facts are indices for the accuracy of the simulation method developed on this work.

8 Conclusion

Since a polycrystalline material consists of grains with different orientations, a micromechanical model of a polycrystalline material should include this grain structure. Therefore, two- and three-dimensional micro components have been modeled including a grain structure. In addition, the presented methods for modeling the grain structure allow investigation of effects such as pores. Studies show

Table 3 Parameters of the simulation performance

	Iterations mean value	SD	Mean cpu time	SD
2D grain structure 1	1350.8	0.7384	2865.8	56.03
2D grain structure 2	1350.7	0.5440	2879.8	70.93
2D grain structure 3	1350.8	0.5956	2022.3	16.04
3D grain structure 1	720.275	0.5541	38,345	1,553

that the grain structure may heavily affect both a component's and therefore the system's behavior. The approach allows examining specific influences to increase the understanding of material, component and system behavior. The consideration of effects coming along with grain structure and tolerances make a contribution to a reliable dimensioning of micro components and systems with distinct grain structures.

Acknowledgments We are grateful for the support provided by German Research Foundation (DFG - Deutsche Forschungsgemeinschaft) within the scope of Collaborative Research Center 499 "Design, Production and Quality Assurance of Molded Micro Components made of Metallic and Ceramic Materials".

References

- Zienkiewicz OC, Taylor RL (2005) The finite element method, 6th edn. Butterworth, London
- Shabana AA (2001) Computational dynamics, 2nd edition, Wiley, London
- Fröhlich A, Weyer S, Metz D, Brückner-Foitt A, Albers A (2001) Investigations on the reliability of FEA calculations on the microscopic scale, technical. In: Proceedings of the 2001 international conference on computational nanoscience, Hilton Head Island, South Carolina (USA)
- McMeeking RM, Hwang SC (1999) A finite element model of ferroelastic polycrystals. *International Journal of Solids and Structures* 36:1541–1556
- Voronoi MG (1908) Nouvelles applications des parametres continus a la theorie des formes quadratiques. *J Reine u Angew Math* 198–287
- Albers A, Metz D (2005) Modeling and validation in design. In: Baltes H, Brand O, Fedder GK, Hierold Ch, Korvink JG, Tabata O, Löhe D, Haußelt J (eds) *Microengineering of metals and ceramics, Part I* Wiley-VCH, Weinheim
- Nygårds M (2003) *Microstructural finite element modeling of metals*. Royal Institute of Technology, Sweden
- Albers A, Metz D (2006) Influence of the microstructure on the strain of micro components, *microsystem technologies*, vol.12. Springer, Heidelberg, pp 685–690
- Stoyan D, Kendall WS, Mecke J (1995) *Stochastic geometry and its applications*, 2nd edn. Wiley, London
- Reher FR (1998) *Simulation der rekristallisation auf der basis orientierter keimbildung und orientierten keimwachstums mittels modifizierter zellularer automaten*. VDI Verlag GmbH, Düsseldorf
- Bäker M (2002) *Numerische methoden in der materialwissenschaft, braunschweiger schriften zum Maschinenbau, Band 8*, Braunschweig, 1. Auflage
- Bunge HJ (1982) *Texture analysis in materials science*. Butterworths, London
- Albers A, Enkler H-G (2007)a *Methods for the Simulation of Micro Components with respect to the Grain Structure*. In: Proceedings of the ASME 2007 international design engineering technical conferences and computers and information in engineering conference, Las Vegas, Nevada, USA
- Albers A, Enkler H-G (2007)b *Modeling of complex three-dimensional grain structures*. Proceedings of the NAFEMS world congress. Vancouver, Canada
- Bathe KJ (1996) *Finite element procedures*. Prentice Hall, Englewood Cliffs, NJ
- Cook RD, Malkus DS, Plesha ME, Witt RJ (2002) *Concepts and applications of finite element analysis*. Wiley, London
- Belytschko T (1976) A survey of numerical methods and computer programs for dynamic structural analysis. *Nucl Eng Des* 37(1):23–34
- Belytschko T (1983) An overview of semidiscretization and time integration procedures. In: Belytschko T, Hughes TJR (eds) *computational methods for transient analysis*. North-Holland, Amsterdam, pp 1–65
- Crisfield MA (1991) *Non-linear Finite element analysis of solids and structures*, vol. 1 and 2, Wiley, UK
- Courant R, Friedrichs KO, Lewy H (1928) Über die partiellen differenzengleichungen der mathematischen physik. *Mathematische Annalen* 100:32–74
- Isaacson E, Keller HB (1966) *Analysis of numerical methods*. Wiley, New York
- Newmark NM (1959) A method of computation for structural dynamics. *ASCE J Eng Mech Div* 5(EM3):67–94
- Hilber HM, Hughes TJR, Taylor RL (1977) Improved numerical dissipation for time integration algorithms in structural dynamics. *Earthq Eng Struct Dyn* 5(3):283–292
- Hughes TJR (1983) Analysis of transient algorithms with particular reference to stability behaviour. In: Belytschko T, Hughes TJR (eds) *Computational methods for transient analysis*. North-Holland, Amsterdam, pp 67–155